JOURNAL OF VIROLOGY, Nov. 2008, p. 10510–10518 Vol. 82, No. 21
0022-538X/08/$08.00+0 doi:10.1128/JVI.01419-08

Region between the Canine Distemper Virus M and F Genes Modulates Virulence by Controlling Fusion Protein Expression▽

Danielle E. Anderson† and Veronika von Messling*

INRS-Institut Armand-Frappier, University of Quebec, Laval, Quebec, Canada

Received 8 July 2008/Accepted 19 August 2008

Morbilliviruses, including measles and canine distemper virus (CDV), are nonsegmented, negative-stranded RNA viruses that cause severe diseases in humans and animals. The transcriptional units in their genomes are separated by untranslated regions (UTRs), which contain essential transcription and translation signals. Due to its increased length, the region between the matrix (M) protein and fusion (F) protein open reading frames is of particular interest. In measles virus, the entire F 5′ region is untranslated, while several start codons are found in most other morbilliviruses, resulting in a long F protein signal peptide (Fsp). To characterize the role of this region in morbillivirus pathogenesis, we constructed recombinant CDVs, in which either the M-F UTR was replaced with that between the nucleocapsid (N) and phosphoprotein (P) genes, or 106 Fsp residues were deleted. The Fsp deletion alone had no effect in vitro and in vivo. In contrast, substitution of the UTR was associated with a slight increase in F gene and protein expression. Animals infected with this virus either recovered completely or experienced prolonged disease and death due to neuroinvasion. The combination of both changes resulted in a virus with strongly increased F gene and protein expression and complete attenuation. Taken together, our results provide evidence that the region between the morbillivirus M and F genes modulates virulence through transcriptional control of the F gene expression.

Measles virus (MeV) and *Canine distemper virus* (CDV) belong to the genus *Morbillivirus*, within the family *Paramyxoviridae*. These viruses are highly contagious and have the capacity to cause severe disease in their respective hosts (1, 7, 8, 26). Morbilliviruses, like all other members of the order *Mononegavirales*, are negative-sense, single-stranded RNA viruses. The morbillivirus genome is composed of six nonoverlapping transcriptional units that produce eight proteins (7). These transcriptional units are separated by untranslated regions (UTRs) consisting of a 3′ region containing transcriptional and translational termination signals for the upstream gene, a nontranscribed three-nucleotide-long intergenic region, and a 5′ region that contains transcription and translation initiation signals for the downstream gene (14). Genes are transcribed by a viral RNA-dependent RNA polymerase (vRdRp) which initiates at the 3′ end of the genome. Using a mechanism known as the stop-start model of transcription (14), the vRdRp pauses at gene junctions, and transcription can then either terminate or continue, creating a polarity of transcription that is maintained throughout infection (21). Thus, genes located closest to the 3′ end of the genome are transcribed in the greatest abundance (12).

Morbillivirus UTRs usually have a combined length of 100 to 200 nucleotides, with the exception of the UTR between the matrix (M) and fusion (F) genes, which reaches to more than 1,000 nucleotides in the case of MeV (9). Since the compact genomic organization and high-coding capacity of genes offer a selective advantage for rapidly replicating RNA viruses (5), the extended length of the morbillivirus M-F UTR is likely to be of functional importance. For MeV, it has been recently demonstrated that the long M-F UTR moderates cytopathogenicity at the expense of replication (28). Furthermore, in vitro studies suggest that the MeV UTR may optimize the level of polymerase available for viral replication (18) and regulate fusion activity (3).

In CDV, the region corresponding to the MeV F 5′ UTR contains several in-frame start codons, resulting in a CDV F 5′ UTR of average length, followed by an unusually long F protein signal peptide (Fsp) (30). Shortening of the Fsp results in increased syncytium formation, indicating that this region regulates the F protein function (30). Further studies have shown that this fusion-enhancing effect is observed only in the context of the Onderstepoort strain vaccine, since shortening of the Fsp originating from the wild-type strain A75/17 did not increase cell-cell fusion (19). Extensive folding and formation of RNA secondary structures due to the high GC content of the CDV M-F region may also contribute to the decrease in F gene expression (15). However, the role of the M-F region in pathogenesis is unknown.

In this study, we examined the contribution of this region and its different functional elements to viral gene expression and virulence. Toward this objective, three recombinant viruses with alterations in the M-F region were produced. After we compared virus growth characteristics and gene and protein expression levels in vitro, their pathogenesis in ferrets was assessed.

MATERIALS AND METHODS

Cells and viruses. VerodogSLAMtag cells (33) and 293 cells (ATCC CRL-1573) were maintained in Dulbecco's modified Eagle's medium (DMEM; Invitrogen) with 5% fetal calf serum (Invitrogen). The parental recombinant CDV 5804PeH (32) and all recombinant mutants constructed in this study were propagated in VerodogSLAMtag cells.

* Corresponding author. Mailing address: INRS-Institut Armand-Frappier, University of Quebec, 531 Boul. des Prairies, Laval, Quebec H7V 1B7, Canada. Phone: (450) 687-5010. Fax: (450) 686-5309. E-mail: veronika.vonmessling@iaf.inrs.ca.

† Danielle E. Anderson's maiden name is Magoffin.

▽ Published ahead of print on 27 August 2008.

Generation of recombinant viruses. The CDV 5804PeH plasmid (32) constituted the basis for the construction of all mutant viruses. Overlap extension PCR (10) was used to produce the recombinant PCR fragments, which were then introduced into the SacII and BsrGI restriction sites of the 5804PeH genome. Three recombinant viruses were generated. To produce the 58utrMF-NPΔF_{106} virus, the M-F UTR was replaced with a duplication of the UTR between the nucleocapsid (N) and the phosphoprotein (P) genes, and the first 106 residues of the Fsp were deleted. An artificial start codon was inserted at position 107 to ensure correct translation of the F gene. For 58utrMF-NP virus, the M-F UTR was replaced with the N-P UTR, but the Fsp remained intact, while for 58ΔF_{106} virus, the M-F UTR remained intact but the first 106 residues of the signal peptide were deleted. The N-P UTR was used as the replacement for the M-F UTR, as it was previously demonstrated that substitution of the MeV M-F UTR with all other counterpart MeV UTRs resulted in a virus rescue of equivalent efficiency (28). The rule of six (2) was respected in all recombinant viruses.

Recombinant viruses were recovered as previously outlined (16). Briefly, semiconfluent 293 cells in six-well plates were transfected with 4 μg of plasmids carrying the recombinant full-length CDV plasmid in combination with 0.5, 0.1, 0.5, and 0.7 μg of MeV N, P, polymerase (L), and T7 polymerase expression plasmids, respectively, using Lipofectamine 2000 (Invitrogen). Two days posttransfection (d.p.i.), cells were trypsinized and seeded onto 100-cm^2 plates together with 5×10^6 VerodogSLAMtag cells. The cocultures were maintained in DMEM containing 5% fetal calf serum until syncytia were observed. Syncytia were then transferred onto fresh VerodogSLAMtag cells to produce virus stocks.

For virus growth curve analyses, VerodogSLAMtag cells were infected at a multiplicity of infection (MOI) of 0.01 50% tissue culture infective dose ($TCID_{50}$) and overlaid with medium containing 0.5% methylcellulose (wt/vol). Samples were harvested daily for 5 days following the infection, and the cell-associated and cell-free titers were determined by limited dilution. Photographs were taken using an Eclipse TE2000-U model compound microscope with a DXM1200F digital camera (Nikon).

Animal experiments and assessment of virulence. Unvaccinated male ferrets (*Mustela putoris furo*) 16 weeks and older (Marshall Farms) were used for all studies. The experiments were performed as described previously (33) and were approved by the institutional animal care and use committee of the INRS-Institut Armand-Frappier. Groups of four to six animals were infected intranasally with 10^5 $TCID_{50}$ of each virus. Body temperature and clinical signs were recorded daily, and blood samples were collected from the jugular vein under general anesthesia twice weekly for the first 2 weeks postinfection and weekly thereafter. Four parameters of virulence were measured and graded. Rash was graded 0 (no rash), 1 (localized rash), or 2 (generalized rash); fever was graded 0 (no fever), 1 (temperature reached above 39°C), or 2 (temperature reached above 40°C); neurological signs were graded 0 (no neurological signs), 1 (behavioral changes), or 2 (paralysis); and weight loss was classified as 0 (0 to 5% loss of day 0 body weight), 1 (5 to 10% loss of day 0 body weight), or 2 (more than 10% loss of day 0 body weight). Cell-associated viremia was quantified by measuring the proportion of infected peripheral blood mononuclear cells (PBMCs) as previously described (34). A Macro-Illumination imaging system (Lightools) was used to monitor enhanced green fluorescent protein (eGFP) expression in ferret organs.

Northern blot analysis. A PCR digoxigenin (DIG) probe synthesis kit (Roche) was used according to the manufacturer's instructions for the generation of the N and F gene-specific DIG-labeled probes, using the 5804PeH genome plasmid as template. Total RNA was isolated from infected cells using an RNeasy RNA extraction kit (Qiagen) in accordance with the manufacturer's protocol. Freshly denatured total RNA (5 μg per sample) was size fractionated in a denaturing morpholinepropanesulfonic acid 1% agarose gel containing formaldehyde and was blotted onto a positively charged nylon membrane (Roche). The blots were first prehybridized with DIG Easy Hyb buffer (Roche) for 1 h at 50°C. Following prehybridization, freshly denatured N or F probes in DIG Easy Hyb buffer (2 μl/ml) were added, and hybridization was carried out at 50°C overnight.

Stringency washes were carried out twice with 2× SSC (1× SSC is 0.15 M NaCl plus 0.015 M sodium citrate), 0.1% sodium dodecyl sulfate (SDS) at room temperature for 5 min and twice with 0.1× SSC, 0.1% SDS, for 15 min at 50°C. Washed membranes were blocked with blocking solution in maleic acid (Roche) for 30 min. Blots were incubated with an anti-DIG alkaline phosphatase antibody (Roche) in blocking buffer at a 1:10,000 dilution for 30 min, washed twice in wash buffer (Roche) for 15 min, and equilibrated in detection buffer (Roche) for 3 min. Detection was performed by incubating blots in CSPD substrate (Roche) for 5 min at room temperature, activating substrate for 10 min at 37°C, followed by exposure on a luminescent image analyzer (Kodak). The mRNA was quantified using Molecular Imaging software (Kodak).

Virus purification. VerodogSLAMtag cells in 100-cm^2 plates were infected with the different viruses at an MOI of 0.01 $TCID_{50}$. Supernatant was harvested when the cytopathic effect reached 80% and clarified by centrifugation at $2,000 \times g$ for 30 min at 4°C. The supernatant was loaded onto a discontinuous sucrose gradient containing 20% sucrose (wt/vol) layered on top of 60% sucrose (wt/vol) and centrifuged at $95,000 \times g$ for 90 min at 4°C. The virus-containing band was harvested in TNE buffer (10 mM Tris-HCl [pH 7.5], 150 mM NaCl, 1 mM EDTA) and pelleted at $95,000 \times g$ for 90 min at 4°C. The purified virus pellet was resuspended in phosphate-buffered saline (PBS), and the viral titer was determined.

Polyacrylamide gel electrophoresis and Western blotting. VerodogSLAMtag cells in 6-well plates were infected with the different viruses at an MOI of 0.01, overlaid with medium containing 0.5% methylcellulose (wt/vol), and incubated at 32°C for 72 h. Cells were washed with PBS, lysed in 100 μl of RIPA buffer (1 mM phenylmethylsulfonyl fluoride, 1% sodium deoxycholate, 50 mM Tris-HCl [pH 7.4], 1% Triton X-100, 0.1% SDS, 150 mM NaCl) on ice for 10 min and then clarified by centrifugation at $17,000 \times g$ for 10 min at 4°C. Cell lysates and infectious virus particles were separated by 10% SDS-polyacrylamide gel electrophoresis and blotted semidry on Immobilon-P polyvinylidene difluoride membrane (Millipore Corporation). Membranes were blocked with blocking buffer (Roche) and sequentially incubated with CDV H, F, and P protein-specific rabbit antipeptide sera (34, 35) and horseradish peroxidase-conjugated secondary antibodies. Proteins were visualized using the ECL Plus Western blotting detection system (GE Healthcare), exposed on a luminescent image analyzer (Kodak), and quantified using Molecular Imaging software (Kodak).

Immunoperoxidase monolayer assay (IPMA). The IPMA was performed as previously described (31). Briefly, VerodogSLAMtag cells in 96-well plates were infected with 5804PeH at an MOI of 0.01 $TCID_{50}$ and incubated at 37°C until the appearance of syncytia. The plates were then washed once with PBS, dried, and fixed at 65°C overnight. CDV-specific antibodies in ferret serum samples were quantified by adding serial twofold dilutions, in duplicate, starting from a dilution of 1:100 in PBS, to the plates, followed by incubation with a peroxidase-labeled, affinity-purified anti-ferret immunoglobulin G (IgG) secondary antibody. Virus-specific staining was visualized after 280 mg/ml 3-amino-9-ethylcarbazole (Sigma) and 0.01% hydrogen peroxide in 50 mM acetate buffer (pH 5.0) was added to the plates. Titers were expressed as reciprocals of the highest antibody dilution at which intracellular viral antigen was detected by light microscopy.

RESULTS

The long M-F region controls replication efficiency and syncytium formation of the recombinant viruses. In morbilliviruses, the region between the M gene stop codon and the F signal peptide cleavage site, which separates the signal peptide from the F_2 subunit of the mature F protein, is up to five times longer than the UTRs between all the other genes. This increased length is due to a longer M 3′ UTR and, depending on the respective virus, either an equally long F 5′ UTR or a combination of a shorter F 5′ UTR and an extended Fsp (Fig. 1). For CDV, the F 5′ UTR is average in length, but the Fsp covers a total of 405 nucleotides, while for MeV, the 574-nucleotide-long F 5′ UTR is followed by a typical signal peptide (Fig. 1). The longer F 5′ UTR is also present in pestes-des-petits-ruminants virus and dolphin morbillivirus, whereas the 5′ UTRs of rinderpest virus and phocine distemper virus are more similar to that of CDV (Fig. 1).

To characterize the role of the long region between M and F in pathogenesis, three recombinant viruses were produced: 58utrMF-NP, in which the M-F UTR was replaced with the N-P UTR; 58ΔF_{106}, in which the first 106 residues of the signal peptide were deleted and a start codon was inserted at position 107 to assure correct F protein translation; and 58utrMF-NPΔF_{106}, a combination of the two previous mutants (Fig. 2A). To evaluate the replication efficiency of the different viruses, growth kinetics were performed. In all cases, the titers in the supernatant were one to two logs lower than the cell-associated

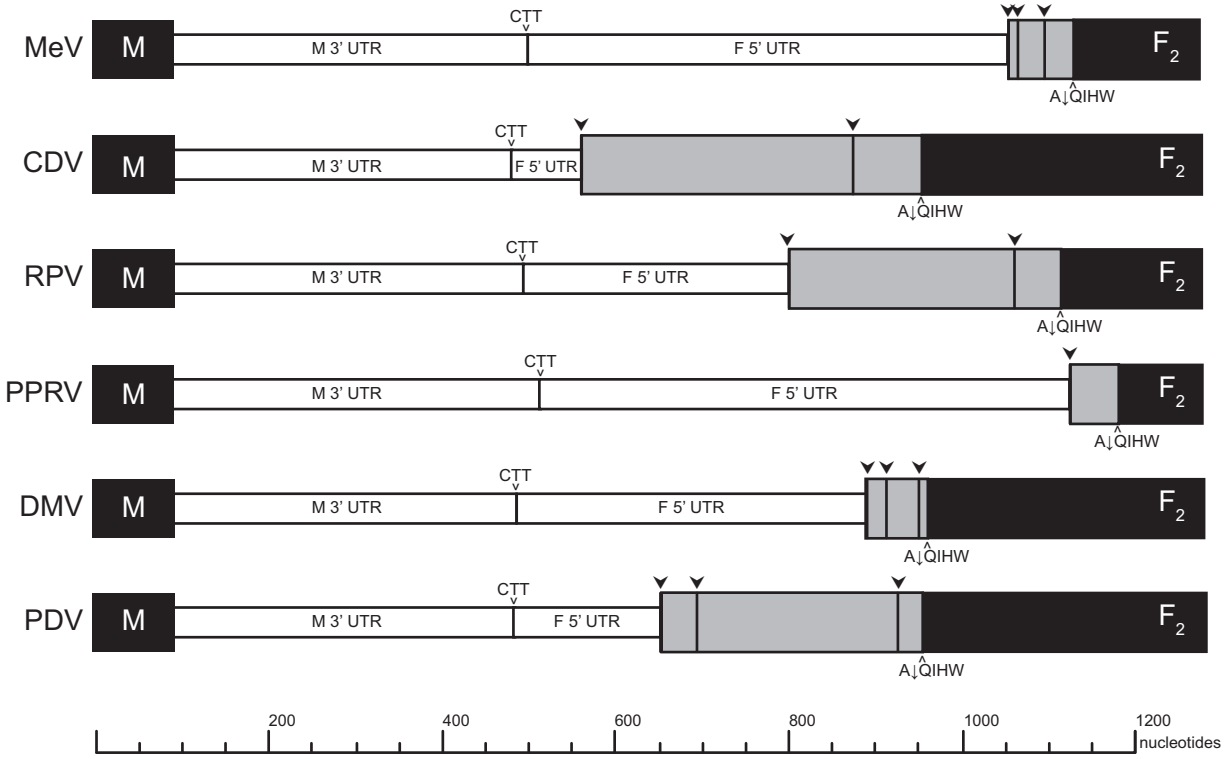

FIG. 1. Schematic diagram of the M-F region in the morbillivirus genome. The M-F region extends from the M gene stop codon to the Fsp cleavage site (A↓QIHW residues). The intergenic region is indicated by the position of the CTT triplet, and the locations of in-frame F start codons are marked by arrowheads. The end of the M protein and the beginning of F_2 subunit of the mature F protein are black, and the putative Fsp is gray. *Measles virus* is the type species of the genus *Morbillivirus* and the Edmonston strain (MeV; GenBank accession no. AF266288) is shown. *Canine distemper virus* (CDV strain 5804P; GenBank accession no. AY386316), *Rinderpest virus* (RPV; GenBank accession no. NC_006296), *Peste-des-petits-ruminants virus* (PRPV; GenBank accession no. NC_006383), *Dolphin morbillivirus* (DMV; GenBank accession no. NC_005283), and *Phocine distemper virus* (PDV; GenBank accession no. D10371) are shown below. Genome components are drawn to scale.

titers (Fig. 2B and C, respectively). $58\Delta F_{106}$ displayed an overall growth pattern similar to that of the parental 5804PeH virus, with the exception of a rapid increase in released virus after infection (Fig. 2B). In contrast, the 58utrMF-NPΔF_{106} and 58utrMF-NP viruses yielded cell-associated and released virus titers that were one and two logs higher, respectively, than that of the 5804PeH virus. To determine the impact of the alterations in the M-F region on the syncytia phenotype, infected VerodogSLAMtag cells were overlaid with methylcellulose. A slight difference in plaque morphology was observed (Fig. 2D). $58\Delta F_{106}$ formed syncytia similar to those of the 5804PeH virus in size and fluorescence intensity, whereas the syncytia associated with 58utrMF-NP and 58utrMF-NPΔF_{106} virus infections were larger and brighter (Fig. 2D). Taken together, the in vitro data demonstrate that the M-F UTR modulates replication and syncytium formation.

M-F UTR is essential for CDV virulence. To determine the role of the region between the M and F genes in CDV pathogenesis, groups of four to six ferrets were infected intranasally with 10^5 $TCID_{50}$ of the different viruses. The deletion of the first 106 residues of the Fsp alone had no effect on the course and outcome of the disease. All animals infected with the $58\Delta F_{106}$ virus developed fever and the characteristic rash starting at 7 d.p.i. and succumbed to the disease within 2 weeks (Fig. 3A and B). Animals inoculated with the 58MF-NP virus, in which the M-F UTR was replaced with the N-P UTR, initially experienced an intermediate disease characterized by a short period of fever and mild generalized rash (Fig. 3A). One-third of these animals recovered completely, while the other two-thirds developed an ascending paralysis at around 4 weeks after infection and had to be euthanized (Fig. 3A and B). However, this reduction in mortality was not statistically significant. In contrast, the group infected with 58utrMF-NPΔF_{106} virus, which lacks the entire M-F region, showed mild signs of disease at between 7 and 10 d.p.i. and survived the infection (Fig. 3A and B). The level of cell-associated viremia peaked in all groups at 7 d.p.i.; however, lethal viruses resulted in titers that were one to two logs higher (Fig. 3C). Survivors cleared the viremia within 3 to 4 weeks after infection, while animals that later succumbed to 58utrMF-NP infection experienced a 100-fold reduction in titer but were unable to completely control and eliminate the virus (Fig. 3C).

To monitor the CDV-specific antibody response, we quantified the total antiviral IgG in serum samples from different time points (Fig. 3D). Animals that succumbed to the disease within 2 weeks were unable to mount a sustained CDV-specific response, as indicated by the stable antibody titers over the course of the infection (Fig. 3D, viruses 5804PeH and $58\Delta F_{106}$). In contrast, animals infected with the 58utrMF-NPΔF_{106} virus experienced a rapid increase in anti-CDV an-

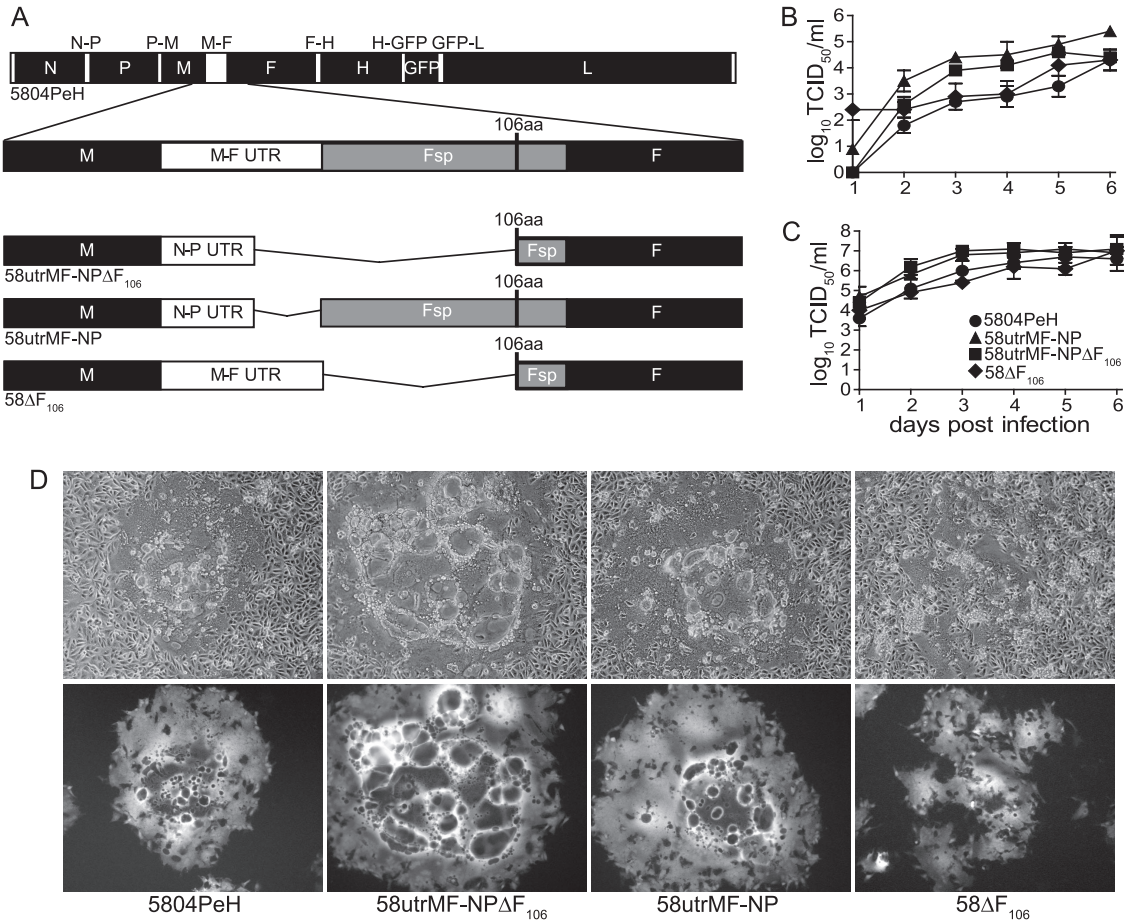

FIG. 2. Growth characterization of recombinant CDVs produced in this study. (A) Schematic drawing of different recombinant viruses. The recombinant 5804PeH genome is drawn to scale. Black and white boxes represent open reading frames and UTRs, respectively. The genes are indicated by their corresponding abbreviations. The M-F region of the recombinant viruses is expanded below. The signal peptide coding region of the F gene (Fsp) is shaded gray. (B and C) Growth curves of the parental 5804PeH virus and the three recombinant viruses in VerodogSLAMtag cells expressed as titers of released (B) and cell-associated virus (C). Cells were infected at an MOI of 0.01, and samples were harvested daily for 5 days. Titers are expressed as $TCID_{50}$. The parental 5804PeH virus is represented by circles, 58utrMF-NP by triangles, 58utrMF-NPΔF_{106} by squares, and 58ΔF_{106} by diamonds. Error bars indicate standard deviations. (D) Syncytium formation in VerodogSLAMtag cells. Cells were infected at an MOI of 0.01 and overlaid with 0.5% methylcellulose. Photographs were taken at 72 h postinfection, using phase contrast (top panels) and fluorescence excitation (bottom panels) at a magnification of ×100.

tibodies as early as 10 d.p.i. Beginning at 21 d.p.i., antibody titers in this group and in the 58utrMF-NP virus survivors were 10-fold higher than those of ferrets that succumbed to 58utrMF-NP virus, coinciding with virus clearance. Altogether, the assessment of the recombinant viruses in ferrets demonstrates that the M-F UTR is an important virulence factor.

UTR replacement alone causes a prolonged disease with neurological involvement in 66% of animals. Ferrets that succumbed to 58utrMF-NP virus infection developed an ascending paralysis at around 28 d.p.i. To determine if the observed neurological signs were related to an ongoing infection of the central nervous system (CNS), the brains were examined at the time of euthanasia. Widespread eGFP expression, located mainly in the brain stem and to a lesser degree in the olfactory bulb, was observed (Fig. 4A and B). The lungs were eGFP negative, indicating that the virus had been mostly cleared from the periphery, which is consistent with the low titer in PBMCs at this time (Fig. 4C and D and Fig. 3C). Brains from animals that recovered completely were examined at 42 d.p.i., and no eGFP expression was detected (data not shown). Thus, inefficient virus clearance was associated with neuroinvasion, suggesting a role for the M-F UTR in the virus-host interactions, leading up to CNS persistence.

Shortening of the M-F region enhances F transcription. Since the UTR, which contains regulatory elements of transcription, had the strongest impact on virulence, the accumulation of F mRNA transcripts produced by the recombinant viruses was compared by Northern blotting. Total RNA isolated from cells infected at an MOI of 0.01 $TCID_{50}$ was extracted and transferred onto nitrocellulose membranes. Membranes were hybridized with DIG-labeled DNA probes specific to the N (Fig. 5A) or F (Fig. 5B) mRNA. Even though some variability was observed, there were no significant differences in the ratio of viral genomic RNA to N mRNA detected for the different mutants (Fig. 5A and B), indicating that the observed effects were based on differences in transcription, not increased

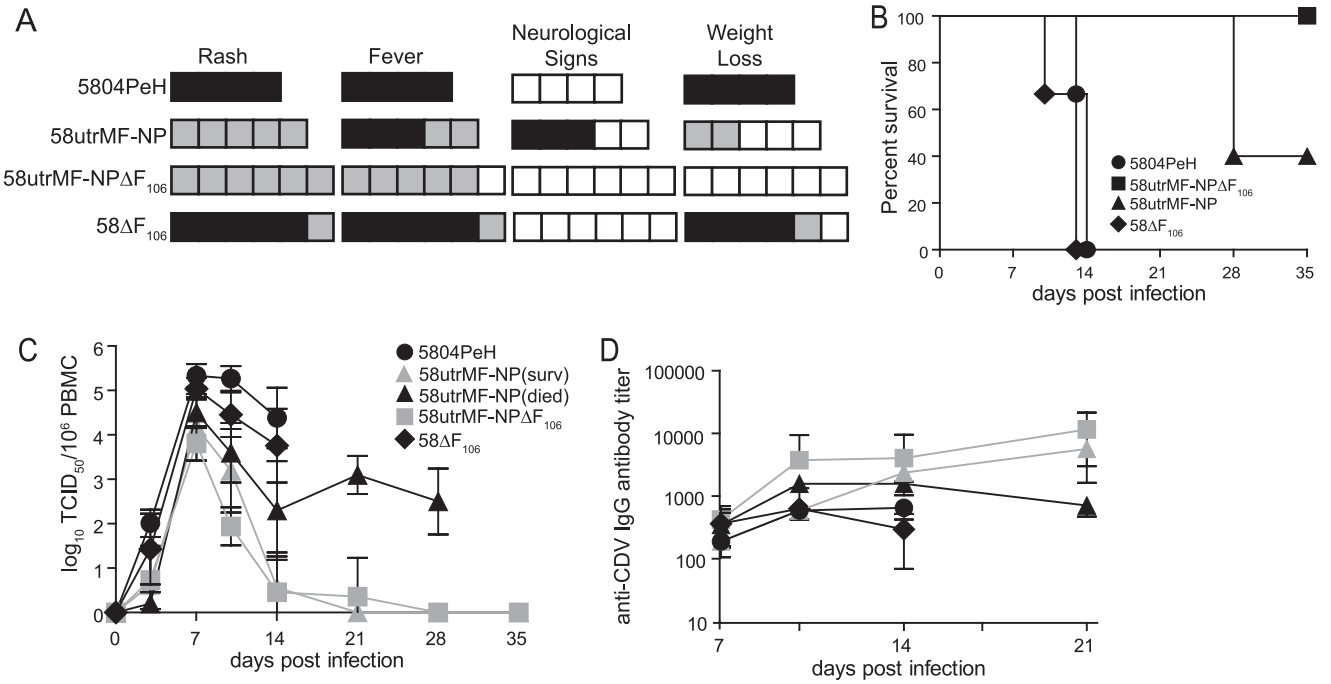

FIG. 3. Virulence of recombinant CDVs in ferrets. (A) A virulence index for the parental and recombinant viruses is shown. Each box represents one animal, and each experimental group contained four to six animals. For the virulence index, black represents the highest score (2), gray represents an intermediate score (1), and white represents the lowest score (0), as specified in Materials and Methods. (B) Survival curve of ferrets infected with the different mutants. Animals were infected with 10^5 $TCID_{50}$ intranasally. Death of an infected animal is indicated by a step down on the graph. (C) The course of cell-associated viremia is displayed as the number of CDV-infected cells per million PBMCs. (D) CDV-specific IgG response in serum samples over the course of the disease. An IPMA was performed, and antibody titers are displayed as reciprocals of the highest antibody dilution at which viral antigen was observed. The 5804PeH virus is represented by black circles, 58utrMF-NPΔF_{106} by gray squares, 58utrMF-NP by black or gray triangles for animals that survived (surv) or died (died), respectively, and 58ΔF_{106} by black diamonds. Error bars indicate standard deviations.

viral genome replication. The relative level of F transcription for each virus was expressed as the ratio of N-to-F mRNA. The mean N/F ratio of the parental 5804PeH and 58ΔF_{106} viruses, which lacks the sequence coding for the first 106 residues of the F signal peptide, was approximately 1 (Fig. 5C), indicating that this region alone has no role in the F gene transcription.

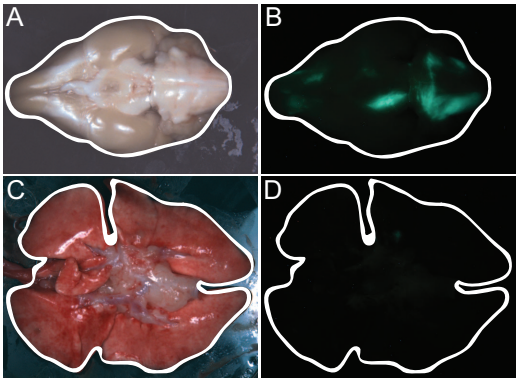

FIG. 4. Macroscopic visualization of eGFP expression in brain and lungs of an animal that succumbed to infection with 58utrMF-NP virus. The contours of the organs are outlined by a white line. (A and B) Ventral view of the brain at the time of euthanasia (28 d.p.i.). (C and D) Ventral view of the lungs at the time of euthanasia (28 d.p.i.). Organs were photographed using phase contrast (A and C) and fluorescence excitation (B and D).

The 58utrMF-NP virus, in which the M-F UTR was replaced with the shorter N-P UTR, yielded a slightly increased N/F ratio of 1.2, while the N/F ratio of the 58utrMF-NPΔF_{106} virus, which lacks the entire M-F region was significantly ($P < 0.005$) higher at 1.9 (Fig. 5C). Since similar analyses of the relative M and H mRNA levels showed no significant differences between the viruses (data not shown), these results indicate that the M-F UTR and Fsp act synergistically and mainly regulate F transcription.

Increased F transcription results in an increased F protein translation and incorporation into mature virions. To assess the effect of the observed increase in F transcription on F protein levels, F protein expression was quantified in infected cells and in infectious virus particles by Western blotting. To analyze the level of F protein expression during infection, VerodogSLAMtag cells were infected with recombinant viruses at an MOI of 0.01 $TCID_{50}$ and overlaid with methylcellulose, and cell lysates were harvested at 72 h p.i. The relative change in F protein expression was expressed as the ratio of F and P protein concentrations. 58utrMF-NPΔF_{106} virus yielded significantly higher ($P < 0.005$) F protein expression levels than the parental virus (Fig. 6A and B, upper panel), while F protein expression levels of the 58utrMF and 58ΔF_{106} viruses were similar to that of the 5804PeH virus (Fig. 6A and B, upper panel). The analysis of relative H protein levels did not show significant differences between the mutant and parent viruses, even though the 58ΔF_{106} virus tended to express slightly less H

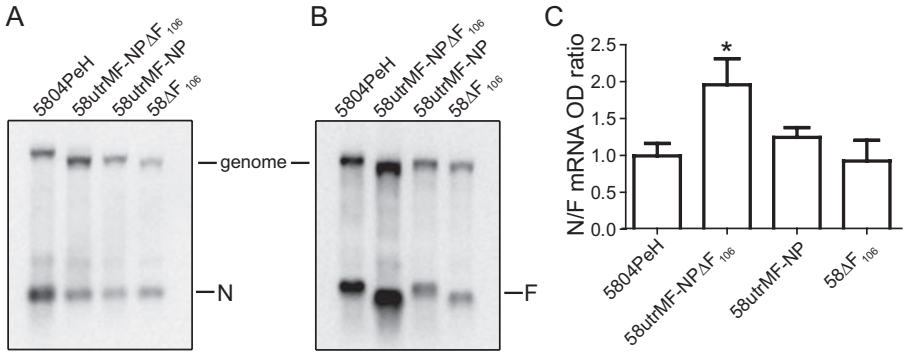

FIG. 5. Effect of the M-F UTR on viral F transcription. (A and B) Northern blot analysis of viral mRNA with DNA probes. Total RNA (5 μg) extracted from VerodogSLAMtag cells infected with 5804PeH virus and the recombinant viruses 58utrMF-NP, 58utrMF-NPΔF_{106}, and 58ΔF_{106} was subjected to Northern blot analysis using DIG-labeled probes. Membranes were hybridized with DIG-labeled DNA probes for CDV N (A) or CDV F (B) mRNA. The genome/antigenome and the position of the N and F mRNAs, respectively, are indicated. (C) Relative quantity of F gene transcription. The ratio of F to N gene expression was calculated for each virus from at least six independent experiments. Error bars represent the standard deviations. Statistical analysis was performed using a one-way analysis of variance with Tukey's multiple comparison test, and the asterisk (*) defines statistically different ($P < 0.005$) samples. Band intensities were determined by densitometry (optical density [OD]) of nonsaturated exposures using Kodak Molecular Imaging software.

protein (Fig. 6A and B, lower panel), confirming that the regulatory function of the M-F region primarily impacts the F protein.

To investigate whether the increased F protein expression levels observed for the 58utrMF-NPΔF_{106} virus resulted in increased F protein incorporation in viral particles, the F protein concentration in infectious purified virions was analyzed. Toward this end, supernatant was collected from infected cells, and viruses were purified through a sucrose gradient. The purified virion suspension was titrated, and 10^5 $TCID_{50}$ of each virus was used for Western blotting analysis. For the same infectious dose, the amount of incorporated F protein relative to the P protein concentration in the 58utrMF-NPΔF_{106} and 58utrMF-NP virions increased up to 140 times, while the F protein content of the 58ΔF_{106} virions remained similar to that of the parental 5804PeH virus (Fig. 6C, top panel).

To determine if this increase was due to a higher percentage of defective particles produced by the viruses lacking the M-F UTR, the relative infectivity of each recombinant virus was calculated by comparing its P protein concentration to that of the 5804PeH virus (Fig. 6C, middle panel). The viruses lacking the M-F UTR, 58utrMF-NPΔF_{106} and 58utrMF-NP, displayed more than 100 times higher relative infectivity, explaining the one to two log increase in virus production and the larger syncytia observed during growth analyses (Fig. 2B and C), whereas the 58ΔF_{106} virions retained a wild-type level of infectivity. While these results do not exclude the possibility of an increased formation of defective particles, they show that by controlling the F gene transcription, the M-F region regulates the amount of F protein available for incorporation into viral particles and thereby the overall infectivity.

DISCUSSION

Compared to the other morbillivirus UTRs, the MeV M-F UTR region is exceptionally long, occupying up to 6.4% of the viral genome (28). As RNA viruses generally do not carry excess genetic information (5), it is likely that this region has a function in the viral life cycle. In this study, we show that the CDV M-F region is essential for virulence in ferrets, since its replacement with a more typical, shorter morbillivirus UTR results in complete attenuation. We demonstrate that this replacement leads to increased F gene transcription that in turn, results in more F protein synthesized. The presence of more F protein in the infected cell leads to increased F protein incorporation into viral particles, a higher infectivity, and larger syncytia. These changes may destroy the delicate balance of immune evasion and dissemination, thus leading to rapid recognition and elimination of the virus by the host's immune system.

The M-F region transcriptionally regulates the F protein expression. Paramyxovirus genes are transcribed in a sequential manner, and transcription of the RNA can either terminate at gene junctions or the vRdRp can reinitiate and continue along the genome (14). Modulation of reinitiation efficiency thus provides a means of transcriptional regulation for negative-stranded RNA viruses. Human parainfluenza virus 1 has a 264-nucleotide-long F 5′ UTR, which decreases F protein expression due to inefficient transcription termination of the upstream M gene, while the Sendai virus F gene start signal reduces reinitiation of transcription by the vRdRp (13). Critical sequences for polyadenylation, located in the last seven nucleotides of the simian virus 5 M 3′ UTR, increase readthrough by the vRdRp during transcription at the M-F gene junction, thereby lowering the level of F protein produced while increasing the transcription of downstream genes (23). However, a recent study with Newcastle disease virus demonstrates that the nonspecific expansion of a UTR results in reduced transcription of the downstream gene, suggesting that specific regulatory elements may not be needed to modulate transcription (36). In the case of MeV, it has been shown that the M 3′ UTR promotes viral replication by increasing the M protein production, while the F 5′ UTR decreases replication and reduces the F protein production and cytopathogenicity (28). The CDV M-F region primarily regulates F gene transcription. It is unclear at this point if the UTR length simply decreases the efficiency of vRdRp reinitiation or if specific

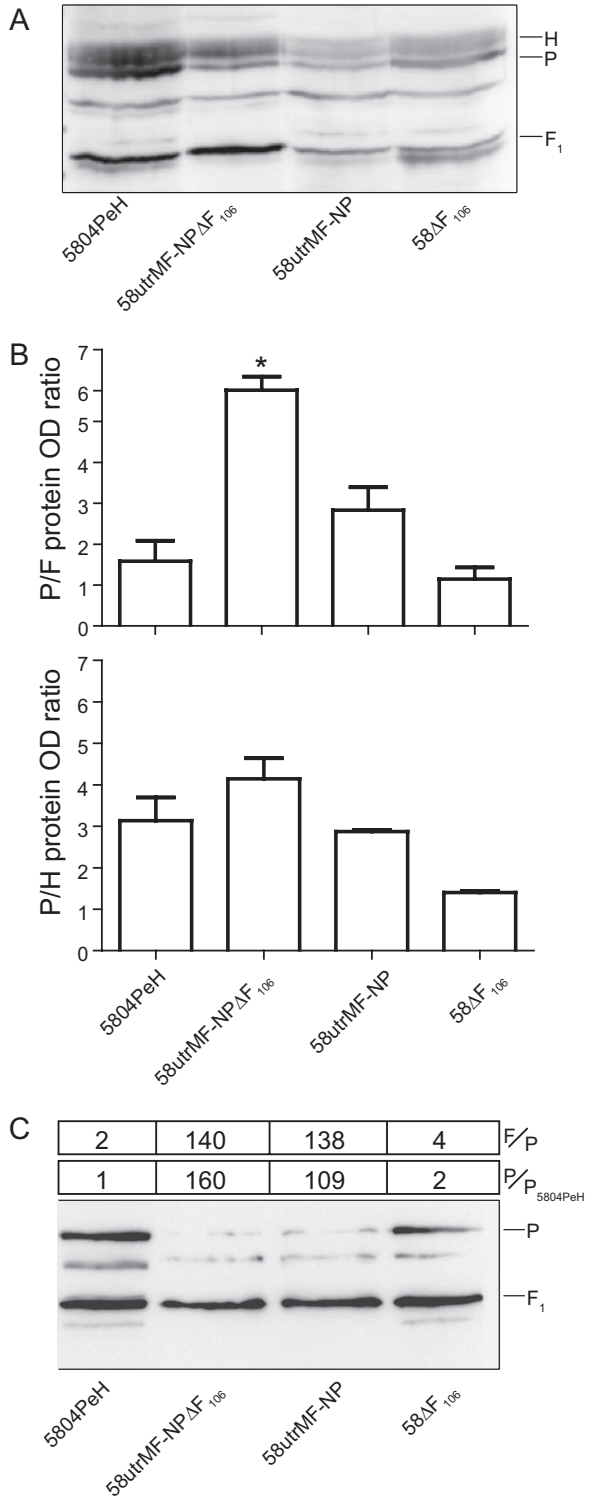

FIG. 6. Effect of M-F UTR on F protein translation and incorporation into infectious virions. (A) Western blot analysis of viral F protein. VerodogSLAMtag cells were infected with the 5804PeH, 58utrMF-NP, 58utrMF-NPΔF_{106}, and 58ΔF_{106} viruses at an MOI of 0.01 and overlaid with 0.5% methylcellulose. Cell lysates were extracted at 72 h postinfection and subjected to Western blot analysis. The membranes were probed with rabbit antipeptide sera specific to the CDV P, F, and H proteins. (B) Normalized F and H protein expression levels. Band intensities of the P, F, and H protein bands were determined by densitometry (optical density [OD]) from nonsaturated exposures, using Kodak Molecular Imaging software. The F and H protein expression levels were normalized by calculating the F/P and H/P ratios for each virus. The graph represents the results from three independent experiments. Error bars indicate the standard deviations. Statistical analysis was performed using a one-way analysis of variance with Tukey's multiple comparison test and the asterisk (*) indicates statistically different ($P < 0.005$) samples. (C) Western blot analysis of F protein incorporation in infectious virions. VerodogSLAMtag cells were infected with the 5804PeH, 58utrMF-NP, 58utrMF-NPΔF_{106}, and 58ΔF_{106} viruses, supernatants were collected, and virions were purified by ultracentrifugation through a 20%/60% discontinuous sucrose gradient. Purified virus titers were determined, and 10^5 $TCID_{50}$ were loaded in each well. Membranes were probed with rabbit antipeptide sera specific to the CDV P and F proteins. The top panel displays the relative F protein incorporation, expressed as a ratio between the OD values of the P and F protein bands of each virus. The middle panel indicates the relative infectivity, as a ratio between the OD of the P proteins of the respective viruses and that of the parental 5804PeH virus.

regulatory elements or secondary RNA structures are involved. However, similar to what has been observed for other paramyxoviruses, this mechanism results in the control of CDV F protein production.

CDV M-F UTR and Fsp act synergistically. The CDV Fsp was originally believed to be a long F 5′ UTR, similar to that of MeV, until its translation was experimentally demonstrated (30). Increasing deletion of the Fsp in the context of the Onderstepoort strain vaccine revealed that this long signal peptide has a fusion-inhibitory function (30). However, in a similar analysis of the Fsp originating from the wild-type strain A75/17, no increase in cell-cell fusion was observed (19). The unchanged syncytium phenotype we observed for the Fsp-deleted virus in this study indicates that the fusion-inhibitory function of Fsp is limited to the vaccine strains. Even though these in vitro results suggest an important role for this region in pathogenesis, our in vivo studies demonstrate that Fsp alone is not essential for virulence, since infection by the virus in which only this region was deleted resulted in a wild-type disease and remained lethal for ferrets. The M-F UTR was also unable to function alone, as demonstrated by the prolonged disease course and decreased lethality of the virus lacking this region. Instead, the M-F UTR and Fsp act synergistically to control F transcription, thereby modulating F protein expression. It remains to be seen if the activity of this region is limited to the RNA level or if the Fsp peptide contributes to the overall control of F protein expression.

Why does increased fitness in vitro correlate with attenuation? We observed that the recombinant CDVs with short N-P UTRs, 58utrMF-NPΔF_{106} and58utrMF-NP, replicated more efficiently in vitro, yielding titers that were one to two logs higher than that of the parental virus. At first glance, it appears counterintuitive that a virus would decrease F transcription and translation at the expense of replication. However, the disease produced by the mutants containing the short N-P UTRs was attenuated, indicating that control of the F protein plays a vital role in CDV pathogenesis.

To establish an infection, viruses need to evade the host's immune system. Most viruses have developed several complementary strategies, including the expression of proteins that

interfere with signal transduction pathways or that mimic immune mediators, the constant alteration of immunodominant envelope glycoproteins, the tight control of replication, and viral gene transcription and translation (6, 29). In the case of paramyxoviruses, viral interference with cellular signal transduction pathways has been extensively characterized (reviewed in reference 11), and the lack of proofreading capacity of the vRdRp explains the rapid emergence of mutants with changed antigenicity (5). In contrast, the contribution of individual gene regulation to immune evasion has received less attention, since the relative amount of mRNA in members of the order *Mononegavirales* is regulated primarily by the gene order and the polar gradient of transcription (14). However, a recent study demonstrates that transfer of the rabies virus glycoprotein originating from a virulent strain into an attenuated strain increases the virulence of an attenuated strain in part by regulating its replication and overall gene expression, thereby enabling the virus to escape immune detection (17, 22). Here, we provide the first indication for transcriptional control of glycoprotein expression as an additional immune evasion mechanism in paramyxoviruses. Even though the underlying virus-host interactions remain to be elucidated, the combination of efficient in vitro replication, rapid induction of an antibody response, and attenuated disease phenotype makes the virus with the deleted M-F region an attractive candidate for the next generation of live-attenuated vaccines and as a vector platform for di- and polyvalent vaccines.

Is inefficient virus clearance a possible cause of morbillivirus neuroinvasion? All morbilliviruses have the potential to cause neurological complications with delayed onset (4, 25). These manifestations are always associated with extensive infection of the CNS and are invariably fatal (27). In MeV infection, individuals with certain immune defects are at high risk of developing measles inclusion body encephalitis several weeks to months after they recover from the acute disease, while infection before the age of two years increases the possibility of subacute sclerosing panencephalitis occurring years to decades later (20, 24). Here, we experimentally reproduce aspects of persistent morbillivirus infection of the CNS in an animal model. Two-thirds of ferrets infected with the 58utrMF-NP virus, in which the M-F UTR was replaced with the N-P UTR, experienced a prolonged disease and developed neurological signs. All animals had extensive infection in the CNS, even though the infection had been almost cleared from the periphery. While much work remains to be done to characterize the underlying mechanisms, our findings suggest that inefficient virus clearance favors neuroinvasion and possibly the establishment of a persistent CNS infection.

ACKNOWLEDGMENTS

We thank Lin-Fa Wang, Roberto Cattaneo, and Urs Schneider for helpful comments on the manuscript. The T7 and MeV protein expression plasmids were a kind gift of Urs Schneider at the Institute for Medical Microbiology and Hygiene, University of Freiburg, Germany. We also thank all laboratory members for continuing support and lively discussions.

This work was supported by grants from the CIHR (MOP-66989), CFI (9488) to V.V.M. and an Armand-Frappier Foundation fellowship to D.E.A.

REFERENCES

1. **Barrett, T., and P. B. Rossiter.** 1999. Rinderpest: the disease and its impact on humans and animals. Adv. Virus Res. **53:**89–110.
2. **Calain, P., and L. Roux.** 1993. The rule of six, a basic feature for efficient replication of Sendai virus defective interfering RNA. J. Virol. **67:**4822–4830.
3. **Cathomen, T., C. J. Buchholz, P. Spielhofer, and R. Cattaneo.** 1995. Preferential initiation at the second AUG of the measles virus F mRNA: a role for the long untranslated region. Virology **214:**628–632.
4. **Cosby, S. L., W. P. Duprex, L. A. Hamill, M. Ludlow, and S. McQuaid.** 2002. Approaches in the understanding of morbillivirus neurovirulence. J. Neurovirol. **8**(Suppl. 2)**:**85–90.
5. **Domingo, E., and J. J. Holland.** 1997. RNA virus mutations and fitness for survival. Annu. Rev. Microbiol. **51:**151–178.
6. **Finlay, B. B., and G. McFadden.** 2006. Anti-immunology: evasion of the host immune system by bacterial and viral pathogens. Cell **124:**767–782.
7. **Griffin, D. E.** 2007. Measles virus, p. 1551–1585. *In* D. M. Knipe, P. M. Howley, D. E. Griffin, R. A. Lamb, M. A. Martin, B. Roizman, and S. E. Straus (ed.), Fields virology, vol. 2. Lippincott Williams & Wilkins, Philadelphia, PA.
8. **Harder, T. C., and A. D. Osterhaus.** 1997. Canine distemper virus: a morbillivirus in search of new hosts? Trends Microbiol. **5:**120–124.
9. **Heider, A., S. Santibanez, A. Tischer, E. Gerike, N. Tikhonova, G. Ignatyev, M. Mrazova, G. Enders, and E. Schreier.** 1997. Comparative investigation of the long non-coding M-F genome region of wild-type and vaccine measles viruses. Arch. Virol. **142:**2521–2528.
10. **Horton, R. M.** 1995. PCR-mediated recombination and mutagenesis. SOEing together tailor-made genes. Mol. Biotechnol. **3:**93–99.
11. **Horvath, C. M.** 2004. Weapons of STAT destruction. Interferon evasion by paramyxovirus V protein. Eur. J. Biochem. **271:**4621–4628.
12. **Iverson, L. E., and J. K. Rose.** 1982. Sequential synthesis of 5′-proximal vesicular stomatitis virus mRNA sequences. J. Virol. **44:**356–365.
13. **Kato, A., K. Kiyotani, M. K. Hasan, T. Shioda, Y. Sakai, T. Yoshida, and Y. Nagai.** 1999. Sendai virus gene start signals are not equivalent in reinitiation capacity: moderation at the fusion protein gene. J. Virol. **73:**9237–9246.
14. **Lamb, R. A., and G. D. Parks.** 2007. Paramyxoviridae: the viruses and their replication, p. 1449–1496. *In* D. M. Knipe, P. M. Howley, D. E. Griffin, R. A. Lamb, M. A. Martin, B. Roizman, and S. E. Straus (ed.), Fields virology, vol. 1. Lippincott Williams & Wilkins, Philadelphia, PA.
15. **Liermann, H., T. C. Harder, M. Lochelt, V. von Messling, W. Baumgartner, V. Moennig, and L. Haas.** 1998. Genetic analysis of the central untranslated genome region and the proximal coding part of the F gene of wild-type and vaccine canine distemper morbilliviruses. Virus Genes **17:**259–270.
16. **Martin, A., P. Staeheli, and U. Schneider.** 2006. RNA polymerase II-controlled expression of antigenomic RNA enhances the rescue efficacies of two different members of the *Mononegavirales* independently of the site of viral genome replication. J. Virol. **80:**5708–5715.
17. **Morimoto, K., D. C. Hooper, S. Spitsin, H. Koprowski, and B. Dietzschold.** 1999. Pathogenicity of different rabies virus variants inversely correlates with apoptosis and rabies virus glycoprotein expression in infected primary neuron cultures. J. Virol. **73:**510–518.
18. **Parks, G. D., K. R. Ward, and J. C. Rassa.** 2001. Increased readthrough transcription across the simian virus 5 M-F gene junction leads to growth defects and a global inhibition of viral mRNA synthesis. J. Virol. **75:**2213–2223.
19. **Plattet, P., P. Cherpillod, D. Wiener, L. Zipperle, M. Vandevelde, R. Wittek, and A. Zurbriggen.** 2007. Signal peptide and helical bundle domains of virulent canine distemper virus fusion protein restrict fusogenicity. J. Virol. **81:**11413–11425.
20. **Plaza, J. A., and G. J. Nuovo.** 2005. Histologic and molecular correlates of fatal measles infection in children. Diagn. Mol. Pathol. **14:**97–102.
21. **Plumet, S., W. P. Duprex, and D. Gerlier.** 2005. Dynamics of viral RNA synthesis during measles virus infection. J. Virol. **79:**6900–6908.
22. **Pulmanausahakul, R., J. Li, M. J. Schnell, and B. Dietzschold.** 2008. The glycoprotein and the matrix protein of rabies virus affect pathogenicity by regulating viral replication and facilitating cell-to-cell spread. J. Virol. **82:**2330–2338.
23. **Rassa, J. C., and G. D. Parks.** 1998. Molecular basis for naturally occurring elevated readthrough transcription across the M-F junction of the paramyxovirus SV5. Virology **247:**274–286.
24. **Rima, B. K., and W. P. Duprex.** 2005. Molecular mechanisms of measles virus persistence. Virus Res. **111:**132–147.
25. **Rima, B. K., and W. P. Duprex.** 2006. Morbilliviruses and human disease. J. Pathol. **208:**199–214.
26. **Roelke-Parker, M. E., L. Munson, C. Packer, R. Kock, S. Cleaveland, M. Carpenter, S. J. O'Brien, A. Pospischil, R. Hofmann-Lehmann, and H. Lutz.** 1996. A canine distemper virus epidemic in Serengeti lions (Panthera leo). Nature **379:**441–445.
27. **Sips, G. J., D. Chesik, L. Glazenburg, J. Wilschut, J. De Keyser, and N. Wilczak.** 2007. Involvement of morbilliviruses in the pathogenesis of demyelinating disease. Rev. Med. Virol. **17:**223–244.
28. **Takeda, M., S. Ohno, F. Seki, Y. Nakatsu, M. Tahara, and Y. Yanagi.** 2005.

Long untranslated regions of the measles virus M and F genes control virus replication and cytopathogenicity. J. Virol. **79:**14346–14354.
29. **Tortorella, D., B. E. Gewurz, M. H. Furman, D. J. Schust, and H. L. Ploegh.** 2000. Viral subversion of the immune system. Annu. Rev. Immunol. **18:**861–926.
30. **von Messling, V., and R. Cattaneo.** 2002. Amino-terminal precursor sequence modulates canine distemper virus fusion protein function. J. Virol. **76:**4172–4180.
31. **von Messling, V., T. C. Harder, V. Moennig, P. Rautenberg, I. Nolte, and L. Haas.** 1999. Rapid and sensitive detection of immunoglobulin M (IgM) and IgG antibodies against canine distemper virus by a new recombinant nucleocapsid protein-based enzyme-linked immunosorbent assay. J. Clin. Microbiol. **37:**1049–1056.
32. **von Messling, V., D. Milosevic, and R. Cattaneo.** 2004. Tropism illuminated: lymphocyte-based pathways blazed by lethal morbillivirus through the host immune system. Proc. Natl. Acad. Sci. USA **101:**14216–14221.
33. **von Messling, V., C. Springfeld, P. Devaux, and R. Cattaneo.** 2003. A ferret model of canine distemper virus virulence and immunosuppression. J. Virol. **77:**12579–12591.
34. **von Messling, V., N. Svitek, and R. Cattaneo.** 2006. Receptor (SLAM [CD150]) recognition and the V protein sustain swift lymphocyte-based invasion of mucosal tissue and lymphatic organs by a morbillivirus. J. Virol. **80:**6084–6092.
35. **von Messling, V., G. Zimmer, G. Herrler, L. Haas, and R. Cattaneo.** 2001. The hemagglutinin of canine distemper virus determines tropism and cytopathogenicity. J. Virol. **75:**6418–6427.
36. **Yan, Y., and S. K. Samal.** 2008. Role of intergenic sequences in Newcastle disease virus RNA transcription and pathogenesis. J. Virol. **82:**1323–1331.